ELSEVIER

Surface Science 479 (2001) 33–42

SURFACE SCIENCE

www.elsevier.nl/locate/susc

STM, STS, and local work function study of Cs/p-GaAs(1 1 0)

T. Yamada, J. Fujii, T. Mizoguchi *

Faculty of Science, Gakushuin University, Mejiro 1-5-1, Toshima-ku, Tokyo 171-8588, Japan

Received 7 December 2000; accepted for publication 24 January 2001

Abstract

Various surface configurations of Cs/p-GaAs(1 1 0) have been studied by scanning tunneling microscopy and scanning tunneling spectroscopy with an interest in relation to the photoelectron emission. The local work function is found to be 4.8, 3.3, and 3.3 eV from clean p-GaAs(1 1 0), Cs one-dimensional (1D) lines (Cs coverage of 0.23 ML), and partially-ordered Cs polygons (Cs coverage of 0.5 ML), respectively. It is understood that only a coherently c(4 × 4)-ordered Cs-polygon surface (Cs coverage of 0.6 and 0.7 ML) can emit photoelectrons due to a sufficient reduction of the local work function down to 1.3 eV to get the negative electron affinity state. The local work function image shows that the boundary of Cs atoms has a lower local work function than at the top of Cs atoms.

Keywords: Photoemission (total yield); Scanning tunneling microscopy; Scanning tunneling spectroscopies; Work function measurements; Photoelectron emission; Alkali metals; Gallium arsenide; Low index single crystal surfaces

1. Introduction

Spin-polarized electron beam experiments belong to one of the most important experimental methods for understanding spin-dependent phenomena in solid state physics and also high energy physics. p-GaAs is now practically used as a spin-polarized photoelectron source [1]. Circularly polarized GaAlAs laser light of 1.58 eV creates a spin dependent excitation of $P_{3/2}$-state valence band electrons to the conduction band at the Γ point. The most crucial point of this method is the surface treatment of the p-GaAs source to get a negative electron affinity (NEA) state in order to emit spin-polarized conduction electrons to the vacuum.

Alkali metals on semiconductor surfaces have been studied for a long time in relation to the metal–semiconductor interface electronic state [2]. In order to investigate the NEA surface, many experimental studies have been performed, including low energy electron diffraction (LEED), Auger electron spectroscopy (AES), and photoelectron spectroscopy (PES) [3–15]. A Cs_2O overlayer, which has the character of an n-type semiconductor (band gap of 2 eV), is considered to be necessary for the NEA state. There is a recipe, the so-called yo–yo treatment, to promote photoelectron emission by alternate deposition of Cs and O_2 on a p-GaAs(0 0 1) surface; however, the mechanism of this procedure is not yet understood. Bands in GaAs bend down approximately 0.4 eV at the interface with Cs_2O, and the work function is reduced from 4.5 to 1.2 eV. In this way, the NEA condition is achieved. Although

* Corresponding author. Tel.: +81-3-3986-0225; fax: +81-3-5992-1029.

E-mail address: tadashi.mizoguchi@gakushuin.ac.jp (T. Mizoguchi).

0039-6028/01/$ - see front matter
PII: S0039-6028(01)00894-9

Cs_2O/p-GaAs(0 0 1) has been used for a practical polarized photoelectron source, no atomic scale information about this surface has been reported. We tried to observe the p-GaAs(0 0 1) surface after various treatments according to the earlier described recipe for a practical photoelectron source. We did not, however, succeed in getting atomic scale images with STM for the (0 0 1) surface as also reported by Bürgler et al. [16].

On the other hand, it was shown by Fujii et al. [10] that photoelectrons could be emitted from Cs/p-GaAs(1 1 0) without oxygen deposition although the emission efficiency is a little bit lower than of the (0 0 1) surface of p-GaAs.

While scanning tunneling microscopy (STM) has been previously used to observe the atomic scale arrangement of Cs atoms on p-GaAs(1 1 0) [17], no study has been reported in relation to the photoemission. The purpose of this study is to find the relation between photoelectron emission and various surface configurations of Cs/p-GaAs(1 1 0). The most important parameter in this perspective is the local work function which has been measured in this study by STM and scanning tunneling spectroscopy (STS) for various Cs coverages on p-GaAs(1 1 0).

2. Experimental

The UHV-STM system comprises an STM head (JEOL-TM-51020STMS) whose limit of measurement is 0.01 nm, an STM controller (JEOL-TM93011000) supplied by JEOL Ltd., an STM chamber with a laser system and a Cs evaporation system, and a preparation chamber with a Au evaporator and a cleaving system, which was constructed in our laboratory. The base pressure of the STM and the preparation chambers were maintained at less than 6×10^{-11} and 2×10^{-10} mbar, respectively. We succeeded to reduce the vibration level of the STM stage to less than 0.01 nm with viton rings, which can damp vibrations above 40 Hz and correctly arranged ring mounts (RM-120-3, Kurashiki Kako Ltd.), which are effective to damp a 25 Hz vibration of the floor.

A p-GaAs(0 0 1) wafer doped with Zn at a concentration of $\sim 10^{19}$ cm^{-3} was cleaved in the UHV chamber to get a clean and flat (1 1 0) surface. Cs atoms were adsorbed on the (1 1 0) surface from a SAES Getters chromate dispenser after a sufficient outgas procedure with a low deposition rate of about 0.08–0.2 ML/min at room temperature in UHV (5×10^{-10} mbar during the deposition). Here, 1 ML (monolayer, ML) is defined as one Cs atom per As atom on the (1 1 0) surface. The Cs coverage was estimated from the STM images and the deposition time. Each Cs polygon was assumed to contain five Cs atoms.

In order to observe photoelectron emission, a 3.0×0.28 mm^2 area of the Cs/p-GaAs(1 1 0) surface, which was biased at -9.2 V, was illuminated with linearly polarized GaAlAs laser light ($\lambda = 780$ nm, 2 mW/mm^2), incident with an angle of 19° relative to the surface normal. The photocurrent was measured with a picoampere meter.

Most STM images were obtained at room temperature in constant current mode with typical set points of 0.130 nA and -1.580 V. Electrochemically etched tungsten tips, which were dipped in 2% HF solution for 10 s to remove the oxide layer [18], were frequently conditioned by high-voltage pulses during tunneling in UHV.

STS was utilized to study the electronic structure of the cleaved, clean p-GaAs(1 1 0) surface and various arrangements of Cs on p-GaAs(1 1 0). *I–V* spectra were taken by cutting off the feed-back loop at a selected position of the image while the sample bias voltage was varied between -2 V to $+2$ V. In order to get information about the local work function, the tunneling current was measured as a function of the separation between the tip and a selected point of the sample surface [19–22]. The local work function images were taken with a lock-in amplifier by modulating the tip-sample separation by ± 0.5 Å at 7.47 kHz, which was higher than the cut-off frequency ($\sim$1 kHz) of the feed-back loop for normal constant mode imaging but within the range of the response frequency ($\leqslant 8$ kHz) of the current amplifier.

3. Results and discussion

Atomic images of Ga and As in the cleaved (1 1 0) surface of p-GaAs from the (0 0 1) wafer are

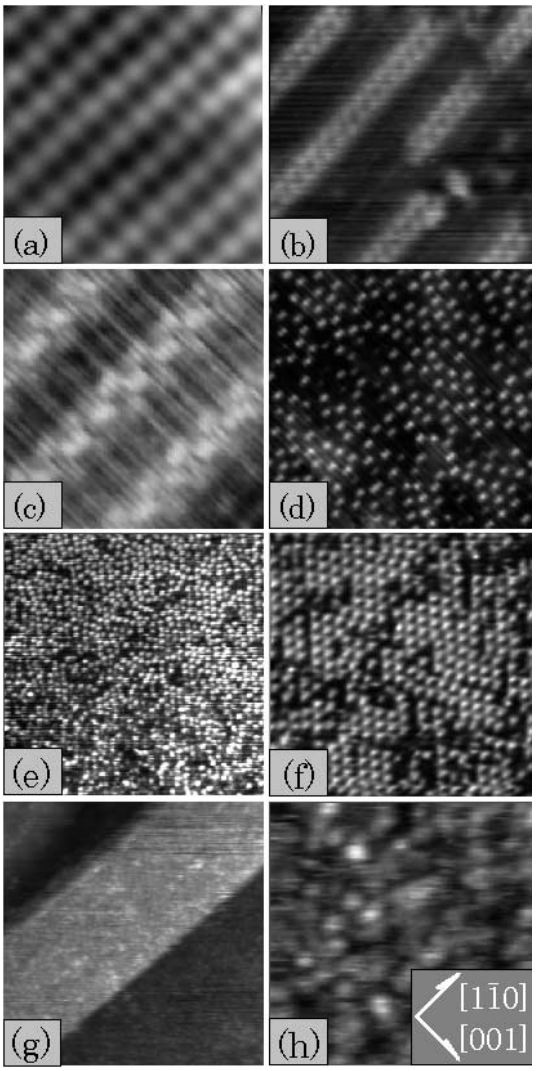

Fig. 1. STM topographic images of Cs/p-GaAs(1 1 0) for different coverages of Cs atoms (sample bias: −1.580 V, tunneling current: 0.130 nA.) The crystallographic direction [1 $\bar{1}$ 0] is oriented 45° counterclockwise from the horizontal. (a) Cleaved p-GaAs(1 1 0) (3×3 nm^2), (b) 0.1 ML Cs (11×11 nm^2), 1D zig-zag line, (c) 0.23 ML Cs (4×4 nm^2), 1D triple line, (d) 0.35 ML Cs (28×28 nm^2), Cs polygons are observed. No photocurrent is detected for cases (a)–(d). (e) 0.5 ML Cs (59×59 nm^2), partially ordered Cs polygons. A photocurrent of 0.18 nA/mm^2 is detected. (f) 0.6 ML Cs (22×22 nm^2), coherently c(4×4)-ordered Cs polygons. A photocurrent of 240 nA/mm^2 is detected. (g) 0.7 ML Cs (65×65 nm^2), layer-by-layer growth of ordered c(4×4) Cs polygons. A photocurrent of 360 nA/mm^2 is detected. (h) Rough surface (40×40 nm^2) of Cs grains of ~5 nm in size is observed when Cs is deposited at a high rate. No photocurrent is detected.

clearly observed at positive bias voltage, +1.795 V, and negative bias voltage, −1.580 V, respectively. The same result has been reported by Feenstra et al. [23].

STM topographic images of Cs atoms on p-GaAs(1 1 0) at various stages of coverage were obtained. Fig. 1(a) shows the cleaved p-GaAs(1 1 0) surface, from which no photocurrent is detected. Then, 0.1 ML of Cs atoms is adsorbed as shown in Fig. 1(b). Cs atoms adsorbed on Ga atoms form a zig-zag one-dimensional (1D) line along the [1 $\bar{1}$ 0] direction. The corrugation of the Cs line is about 1 Å from the As surface, and the corrugation in the line is about 0.2–0.3 Å. No photoemission is observed at this stage.

Fig. 1(c) shows a surface covered by 0.23 ML Cs. One more Cs line starts beside the zig-zag line making a line of three rows of Cs atoms along the [1 $\bar{1}$ 0] direction on the (1 1 0) surface. The arrangement of Cs atoms is c(2×2) for the substrate As lattice, where the central Cs atoms are observed to be 0.4 Å higher than the Cs atoms in the side rows in the constant current imaging mode as shown in Fig. 2. This height difference is considered to be apparent because the tunneling current will flow more easily to the Cs atom in the central row if the tip–sample separation is kept constant. The tunneling current is estimated to increase by a factor of 2.1 from the observed decay rate, $\kappa = 1.85$ Å^{-1} for a Cs 1D line. No photoemission is observed at this stage.

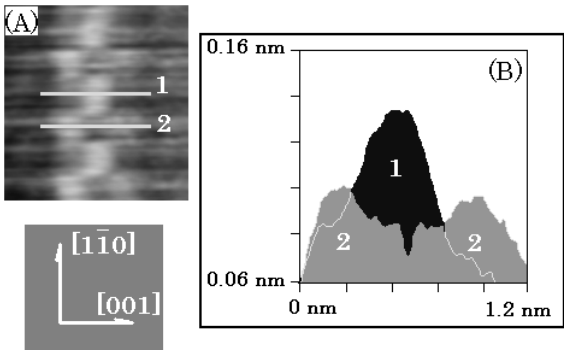

Fig. 2. The observed height of the triple row Cs line in a constant current image (0.130 nA, sample bias −1.580 V). (A) STM topographic image (2.5×3.0 nm^2) of a Cs 1D triple line. (B) The line profiles corresponding to the white lines in (A).

Increasing the coverage of Cs, the Cs lines becomes longer and the number of lines increases. Above a coverage of 0.25 ML, the Cs lines start to contact each other, and the lines transform into Cs polygons. At 0.35 ML Cs coverage, the 1D Cs lines disappear, and Cs polygons cover the (1 1 0) surface as shown in Fig. 1(d). A Fourier-transform-STM image suggests that Cs polygons start to make ordering. No photoemission is observed at this stage.

At about 0.5 ML Cs on the (1 1 0) surface, the Cs polygons adopt partial ordering as shown in Fig. 1(e). At this stage, a weak photocurrent ($\sim$0.18 nA/mm^2) is detected. Fig. 1(f) shows a surface covered with about 0.6 ML Cs. A coherent c(4 $\times$ 4) two-dimensional (2D) long range ordering of Cs polygons covers the (1 1 0) surface.

In Fig. 3(A) an enlarged image of the ordered Cs polygons is shown. Whitman et al. [17] proposed that each polygon contains five Cs atoms, which are arranged in a unit cell as shown in Fig. 3(C). Although Cs atoms inside the polygon cannot be separated in our observation, it seems to us more plausible, from the observed total shape of each polygon, that the Cs atoms are arranged as shown in Fig. 3(B). This configuration can be understood as the alternative arrangements of the half filled and 3/4 filled 1D Cs lines with respect to the As lattice along the [1 $\bar{1}$ 0] direction.

The photocurrent drastically increases up to 240 nA/mm^2 for this c(4 $\times$ 4)-ordered Cs-polygon surface. The photocurrent decays by 1/3 with irradiation of laser light for 1 min, but becomes more stable afterwards.

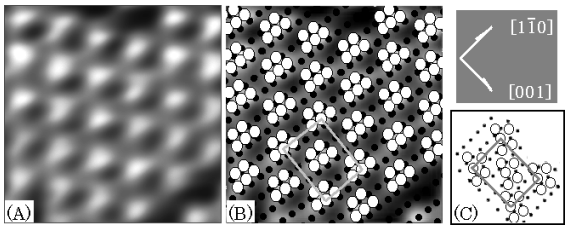

Fig. 3. (A) STM topographic image (7.5 $\times$ 7.5 nm^2) of 2D c(4 $\times$ 4)-ordered Cs polygons (sample bias: $-$1.580 V, tunneling current: 0.130 nA). (B) Although Cs atoms inside the polygon cannot be separated in our observation, it seems to us more plausible from the observed total shape of each polygon. Cs atoms (white circles) are arranged in (A) with respect to substrate As atoms (small black spots). (C) The reported arrangement of Cs atoms in a unit cell of Cs polygons by Whitman et al. [17].

When the (1 1 0) surface was covered with about 0.7 ML Cs, we observed layer-by-layer growth of c(4 $\times$ 4) 2D-ordered Cs polygons as shown in Fig. 1(g). The height of the layer is 3.2 and 7 Å, which is roughly equal to an atomic diameter of the Cs atom and twice that, respectively. The photocurrent reaches 360 nA/mm^2 at this stage. A c(4 $\times$ 4) 2D-ordered Cs polygon-growth on the stepped p-GaAs(1 1 0) surface was also observed, for which the step height was equal to the step height (2 Å) of p-GaAs(1 1 0).

When Cs atoms are deposited with higher deposition rates, they do not grow layer-by-layer and the surface becomes very rough with Cs grains of $\sim$5 nm in size as shown in Fig. 1(h). No photocurrent is observed for this thick Cs surface.

All topographic images in Fig. 1 were taken without laser light illumination. Although no photocurrent by electron emission is detected from the Cs 1D lines, there is a clear enhancement of the tip–sample distance in the constant current mode (roughly 0.1 nm) at Cs lines as shown in Fig. 4 when 0.5 mW/mm^2 laser light ($\lambda = 780$ nm) illumination is turned on. The tunneling current to the Cs 1D line with photoexcitation is estimated to increase by a factor of 6 from the observed decay rate, $\kappa = 1.85$ Å^{-1} for a Cs 1D line.

In Fig. 5, the results of I–V spectra measured at different surface configurations of Cs/p-GaAs(1 1 0) are shown. In bulk p-GaAs, the band gap at the Γ point is 1.43 eV at room temperature, and the Fermi level is very close to the top of the valence band. The I–V spectrum obtained on the cleaved p-GaAs(1 1 0) surface indicates that the bottom of the conduction band is about 1.4 eV above the Fermi level. The top of the valence band is about 0.05 eV below the Fermi level, which suggests that the band bending for the p-GaAs(1 1 0) surface is quite small. At the position of the Cs line or Cs polygon in Fig. 1(b)–(g), the band gap is reduced to 0.9–1.2 eV. The Fermi level is 0.45–0.6 eV below the bottom of the conduction band, i.e., at the center of the band gap. These adsorbed Cs overlayers have characteristics of semiconductors without any

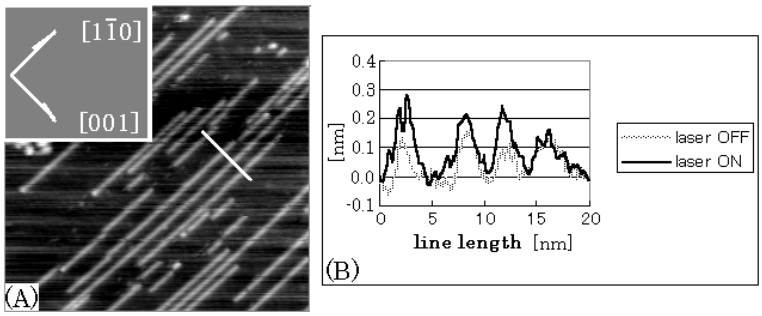

Fig. 4. Enhancement of the tip–sample distance (B) on the Cs lines (A) in the constant current mode (0.130 nA, sample bias: −1.580 V) shown when the laser illumination (0.5 mW/mm^2) is turned on.

explicit differences. Whitman et al. [17] reported that the band gaps of Cs 1D zig-zag lines on n-GaAs(1 1 0), Cs 1D-triple lines on p-GaAs(1 1 0), and a c(4 × 4) 2D-ordered Cs-polygon overlayer were 1.10, 0.65 and 0.6 eV, respectively. The thick Cs surface with Cs grains of ~5 nm in size (Fig. 1(h)) has a metallic characteristic without a band gap.

In order to get information on the local surface work function, the tunneling current is measured with varying tip–sample separation S [19,24–29]. The tunneling current decays with S as

$$I = I_0 \exp[-\kappa S] \quad (1)$$

The decay rate κ is related to an effective local potential barrier height ϕ_A via,

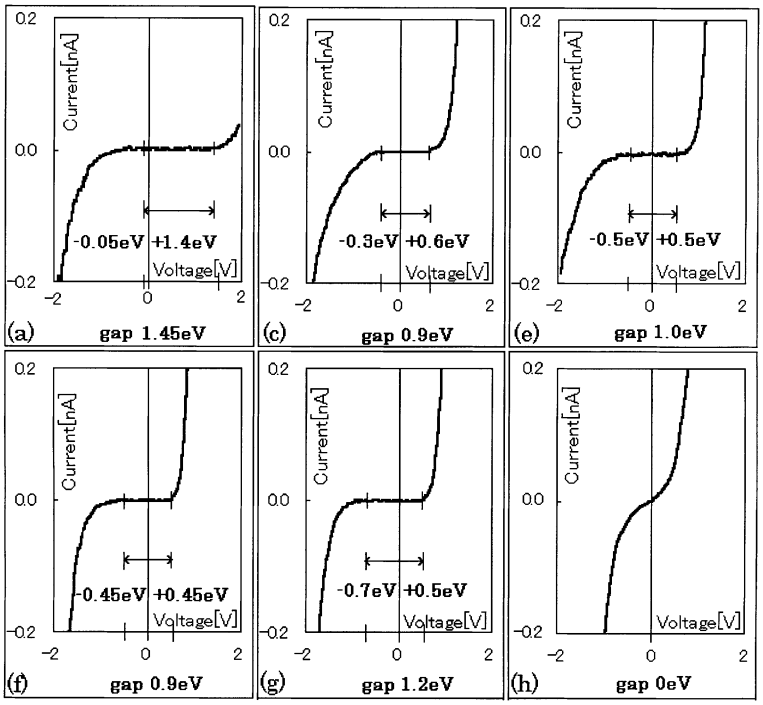

Fig. 5. The tunneling current versus bias voltage (I–V spectra) measured at (a) p-GaAs(1 1 0), (c) Cs 1D triple line, (e) partially ordered Cs polygons, (f) c(4 × 4) 2D-ordered Cs polygons, (g) ordered Cs-polygon layer, and (h) Cs metallic thick surface. (a), (c), (e), (f), (g), and (h) correspond with those in Fig. 1, respectively.

$$\kappa = \sqrt{32\pi^2 m\phi_A}/h \quad (2)$$

where m is the electron mass and h is the Plank constant. Here ϕ_A is the averaged value of the work function of the sample and the tungsten tip, i.e.,

$$\phi_A = (\phi_{tip} + \phi_{sample})/2 \quad (3)$$

In order to calibrate the work function of our tungsten tip, we prepared clean a Au film of 100 nm thick on p-GaAs(1 1 0) and Si(1 1 1), and annealed at over 1300 K to get an ordered (1 1 1) surface. The observed barrier height between Au(1 1 1) and our tungsten tip was 4.3 ± 0.3 eV. Using the reported value of the work function of Au(1 1 1) surface in the literature, 5.38 eV [30], the work function of our tungsten tips was deduced to be 3.2 eV.

In Fig. 6, the tunneling current, in logarithmic scale, was measured as a function of ΔS at all the observed Cs/p-GaAs surfaces. Here, ΔS is the shift of tip–sample distance from a tip-approaching position with tunneling current 0.130 nA and sample bias -1.580 V, i.e., I is 0.130 nA at $\Delta S = 0$,

		κ	ϕ_{sample}
(a)	○	2.05 ± 0.07 Å^{-1}	4.8 ± 0.27 eV
(c)	□	1.85 ± 0.07 Å^{-1}	3.3 ± 0.25 eV
(f)	△	1.54 ± 0.07 Å^{-1}	1.3 ± 0.21 eV

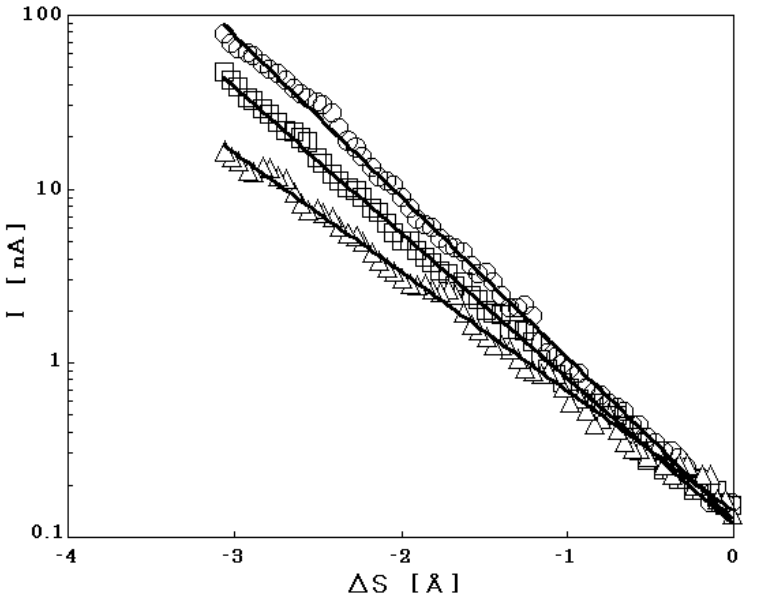

Fig. 6. The tunneling current (I) in logarithmic scale versus ΔS from (a) p-GaAs(1 1 0) (○), (c) Cs triple line (□), and (f) c(4 × 4) 2D-ordered Cs polygons (△). (a), (c), and (f) correspond with those in Fig. 1, respectively. Here, ΔS is the shift of tip–sample distance from a tip-approaching position with tunneling current 0.130 nA and sample bias -1.580 V, i.e., I is 0.130 nA at $\Delta S = 0$, and $\Delta S < 0$ means that the tip approaches to the sample. The decay rate κ is obtained from these plots, and then the local work function ϕ_{sample} is derived using Eqs. (2) and (3).

and $\Delta S < 0$ means that the tip approaches to the sample. By way of illustration, three typical spectra are shown in Fig. 6 for a cleaved clean p-GaAs (1 1 0) (Fig. 1(a)), the Cs triple line (Fig. 1(c)), and the c(4 × 4)-ordered Cs polygons (Fig. 1(f)).

The decay rate κ is deduced from the slope of the $\log I$ versus ΔS plot to be 2.05 ± 0.07 Å^{-1} for p-GaAs(1 1 0). The κ for the Cs zig-zag line, the Cs triple line, the Cs polygons, and the partially ordered Cs polygons coincide within the experimental error to the same value of 1.85 ± 0.07 Å^{-1}. The κ for the c(4 × 4)-ordered Cs polygons is found to be 1.54 ± 0.07 Å^{-1}. The local work function of each configuration is calculated by Eqs. (2) and (3). It is deduced to be 4.8 ± 0.27 eV for the clean p-GaAs(1 1 0) (Fig. 1(a)). The local work functions at the position of the Cs line or Cs polygon in Fig. 1(b)–(e) have the same value of 3.3 ± 0.25 eV. Only the local work function of c(4 × 4) 2D-ordered Cs polygons on the (1 1 0) surface (0.6 ML Cs) (Fig. 1(f)) is found to be remarkably reduced down to 1.3 ± 0.21 eV, which is less than the band gap of bulk p-GaAs, i.e., 1.43 eV.

In Fig. 7, the local work function images ((A-2) and (B-2)) are shown together with normal topographic images for the Cs 1D line (A-1) and the coherently c(4 × 4)-ordered Cs polygons (B-1) on p-GaAs(1 1 0). The region of Cs 1D lines, which are bright in the topographic image (A-1), clearly corresponds to the dark region in (A-2) where the local work function is lower. The noise of the local work function image is reduced by the lock-in technique, and the atomic image becomes clearer than in the normal topographic imaging mode.

It is quite interesting to point out that the top of the Cs atoms is brighter in the dark region of the Cs lines in the local work function image (Fig. 7(A-2)). For the coherently c(4 × 4)-ordered Cs polygons, the boundary between the Cs polygons is darker than the top of the polygons in Fig. 7(B-2), where white particles in the polygons would correspond to individual Cs atoms although the resolution and the signal to noise ratio is critical. It should be noted that photoelectrons emerge from the boundary of Cs atoms where the local work function is lower than that at the top of Cs atoms.

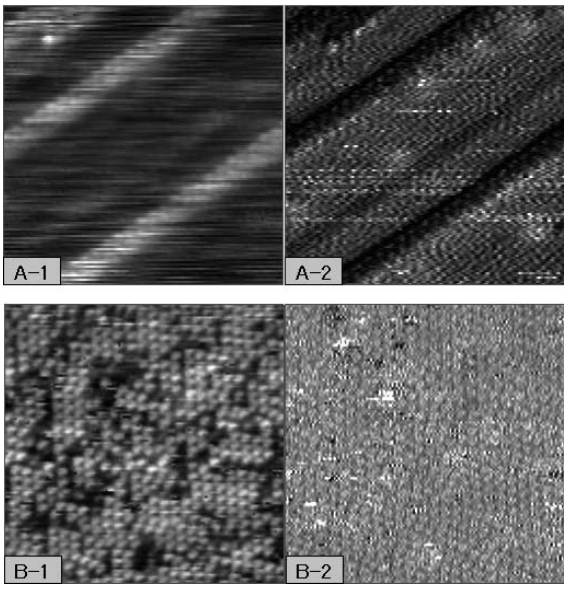

Fig. 7. Topographic atomic image (A-1) and the local work function image (A-2) for a Cs 1D-line (19 × 19 nm^2) surface. Topographic atomic image (B-1) and the local work function image (B-2) for a c(4 × 4) 2D-ordered Cs-polygon surface (40 × 40 nm^2). In the local work function images, the darker part has a lower work function. In (A-2) and (B-2), one pixel corresponds with 0.156 and 0.312 nm, respectively.

A phenomenological explanation why the boundary of Cs atoms shows a lower work function may be as follows. In constant current mode, the path of the tip follows the corrugation of Cs atoms more sensitively for a high constant tunneling current than for a low tunneling current for which the path becomes smooth and flat because the tip is further away from the surface. This means that the derivative ($\Delta \ln I/\Delta S$), i.e., κ becomes lower at the boundary of Cs atoms, where the path is concave, than at the top of Cs atoms as shown in Fig. 8.

In Fig. 9, the results of the I–V and I–S experiments are summarized in an energy band scheme together with STM images for the cleaved p-GaAs(1 1 0), the Cs 1D zig-zag line, and the coherently c(4 × 4)-ordered Cs-polygon surface. It is understood that the photoexcited conduction electrons in p-GaAs can be emitted from the coherently c(4 × 4)-ordered Cs-polygon surface only thanks to the remarkable reduction of the local

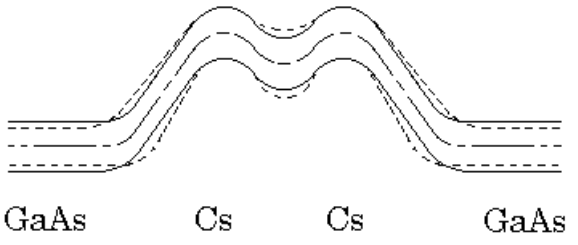

Fig. 8. A schematic illustration of the local work function images (Fig. 7). The dash-dotted line reveals the path of the tip for $I_0 = 0.130$ nA. The two solid lines reveal paths of the modulated tip ($\Delta S = \pm 0.5$ Å). The upper and lower dotted lines reveal paths of the tip for $\ln I_1 = \ln I_0 - 0.925$ and $\ln I_2 = \ln I_0 + 0.925$, respectively. The separation between the dotted lines is inversely proportional to the derivative $\mathrm{d} \ln I/\mathrm{d}S$.

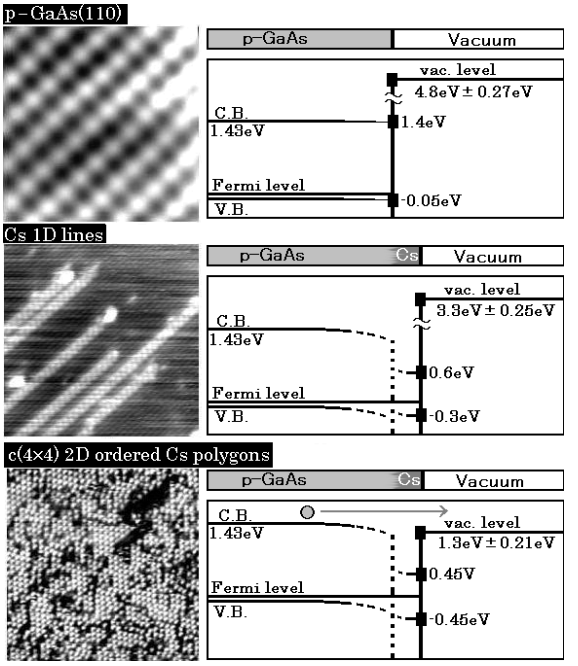

Fig. 9. The energy band diagrams for the photoemission-process at p-GaAs(1 1 0), the Cs 1D line, and the c(4 × 4) 2D-ordered Cs-polygon surface. The band gap in the p-GaAs is 1.43 eV at room temperature [1]. Square marks represent our STS results.

work function down to 1.3 ± 0.21 eV, which is less than the bottom of the conduction band in p-GaAs.

In Fig. 10, the local work function, the top of the valence band, the bottom of the conduction band, and the observed photocurrent are plotted versus the coverage of Cs on p-GaAs. The quantum efficiency (photoelectrons/photons) is so low, of the order of 10^{-3} in our observation, that the photocurrent indicates only the onset of the photoemission. It should be noted that the local work function of Cs/p-GaAs(1 1 0), which is measured at the position of the Cs line or Cs polygon, must be distinguished from the averaged work function, which is usually treated as a function of the coverage of Cs, θ, on the surface.

There is a general tendency that the averaged work function of the surface adsorbed by alkali atoms decreases linearly with increasing coverage of alkali atoms on the surface. The local work functions at the Cs configurations of Fig. 1(b)–(e) are observed to reduce to 3.3 eV, which gives the averaged work function $4.8(1-\theta) + 3.3\theta$ (eV). Further reduction of the local work function occurs down to 1.3 eV for the coherently c(4 × 4)-ordered Cs-polygon surface whose coverage is 0.6 ML.

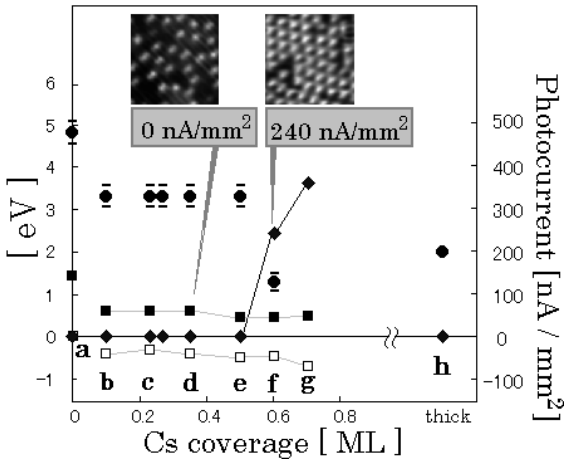

Fig. 10. The local work function (●), the top of the valence band (□), the bottom of the conduction band (■), and the observed photocurrent (♦) are plotted versus the coverage of Cs on p-GaAs. a–h correspond with those in Fig. 1, respectively. The local work function, the top of the valence band, and the bottom of the conduction band of Cs/p-GaAs(1 1 0) are measured at (a) the (1 1 0) surface, (b–g) the position of Cs line or Cs polygon, and (h) the Cs metallic surface. Although we did not measure the local work function at the Cs thick surface, the work function of Cs bulk [2] is shown at the thick Cs coverage.

The averaged work function of a metal has been interpreted by a simple jellium model [31,32]. The reported calculation of electronic states of adsorbed Na atoms on jellium [33] shows that the density of electrons is reduced in the region of the vacuum side of the adsorbed atoms and increases in the intermediate region between the adsorbed atoms and the surface of jellium. This charge transfer, due to the bonding mixture between electron orbitals of alkali atoms and those of substrate atoms, is thought to reduce the averaged work function.

At full coverage, the valence electrons of adsorbed atoms are thought to form energy bands through direct mixing of bonding orbitals. The local situation of Cs polygons or even Cs lines where Cs atoms are lined closely may correspond to the full coverage in the calculation of the uniform square lattice where the nearest neighbor distance between Na atoms is defined to be 8 a.u. (4.24 Å) at full coverage. It is interesting to note that the density of electrons is reduced rather between alkali atoms than at the top of them in the region of the vacuum side at full coverage. This means that the local work function is lower between Cs atoms rather than at the top of them, which may be an additional explanation of our observation that the boundary of Cs atoms seems darker in the local work function images (Fig. 7(A-2) and Fig. 7(B-2)).

The calculated dipole moment per Na adatom decreases with coverage and the averaged work function reaches a minimum at half coverage and increases with coverage beyond the minimum. This tendency suggests that the local work function should increase with a coverage of more than half. The observed local work function, however, decreases drastically at a coverage of 0.6 ML, which may correspond to the full coverage in the square lattice calculation. This remarkable reduction of the local work function must be related to the coherent ordering of Cs polygons. There must be some mechanism to enhance the reduction of the local work function induced by the coherent ordering of Cs polygons.

The ordered polygons induce a perturbation potential, which opens up the additional band gap at the zone boundary of new the Brillouin zone, which corresponds to a c(4×4) super-lattice in the 2D band of surface electrons. There may be a possibility with this mechanism that the charge transfer and then the reduction of the local work function are enhanced so as to reduce the total energy of the electronic system.

4. Conclusion

The local work function for various surface configurations of Cs/p-GaAs(1 1 0) was found to be 4.8, 3.3, 3.3 eV for the clean p-GaAs(1 1 0), Cs 1D lines (Cs coverage of 0.1 and 0.23 ML), and partially-ordered Cs polygons (Cs coverage of 0.5 ML), respectively. It was understood that only the coherently c(4×4)-ordered Cs-polygon surface (Cs coverage of 0.6 and 0.7 ML) can emit photoelectrons due to a sufficient reduction of the local work function down to 1.3 eV to get the NEA state.

Acknowledgements

We would like to express our sincere thanks for valuable discussions to Prof. Dr. Herman van Kempen, M.M.J. Bischoff, and R. de Kort, and to Dr. M. Tokii and Dr. A. Keen for the preparation of the manuscript. We appreciate the support by the High Tech Research Center from the Ministry of Education Science, Sports and Culture.

References

[1] D.T. Pierce, et al., Appl. Phys. Lett. 26 (1975) 670.
[2] J.S. Escher, Semiconductor and Semimetals, vol. 15, 1981 (Chapter 3).
[3] A. Simon, E. Westerbeck, Angew. Chem. Int. Ed. 11 (1972) 1105.
[4] C.Y. Su, W.E. Spicer, I. Lindau, J. Appl. Phys. 54 (1983) 1413.
[5] D.T. Pierce, R.J. Celotta, G.-C. Wang, W.N. Unertl, A. Galejs, C.E. Kuyatt, S.R. Mielczarek, Rev. Sci. Instrum. 51 (1980) 478.
[6] G. Lengel, J. Harper, M. Weimer, Phys. Rev. Lett. 76 (1996) 4725.
[7] H. Sonnenberg, Appl. Phys. Lett. 14 (1969) 289.
[8] J.J. Uebbing, L.W. James, J. Appl. Phys. 41 (1970) 4505.

[9] J. Derrien, F.A. D'avitaya, Surf. Sci. 65 (1977) 668.
[10] J. Fujii, K. Tamura, S. Ishizuka, T. Sato, T. Mizoguchi, Surf. Rev. Lett. 5 (1998) 305.
[11] K.-J. Chao, A.R. Smith, C.-K. Shih, Phys. Rev. B. 53 (1996) 6935.
[12] M.G. Clark, J. Phys. D. Appl. Phys. 8 (1975) 535.
[13] R.L. Bell, Negative Electron Affinity Devices, 1973, p. 39.
[14] V.L. Alperovich, A.G. Paulish, A.S. Terekhov, Phys. Rev. B 50 (1994) 5480.
[15] W.E. Spicer, I. Lindau, P. Skeath, C.Y. Su, P. Chye, Phys. Rev. Lett. 44 (1980) 420.
[16] D.E. Bürgler, C.M. Schmidt, D.M. Schaller, F. Meisinger, R. Hofer, H.J. Güntherodt, Phys. Rev. B 56 (1997) 4149.
[17] L.J. Whitman, J.A. Stroscio, R.A. Dragoset, R.J. Celotta, Phys. Rev. Lett. 66 (1991) 1338.
[18] T. Kawagoe, N. Kondoh, Y. Jimma, T. Kotaki, A. Itoh, Jpn. J. Appl. Phys. 38 (1999) 3816–3819.
[19] R. Wiesendanger, Scanning Probe Microscopy and Spectroscopy, Cambridge University Press, Cambridge, 1994.
[20] N. Garcia, C. Ocal, F. Flores, Phys. Rev. Lett. 50 (1983) 2002.
[21] J.F. Jia, K. Inoue, Y. Hasegawa, W.S. Yang, T. Sakurai, Phys. Rev. B 58 (1998) 1193.
[22] G. Binnig, H. Rohrer, Ch. Gerber, E. Weibel, Appl. Phys. Lett. 40 (1982) 178.
[23] R.M. Feenstra, J.A. Stroscio, J. Tersoff, A.P. Fein, Phys. Rev. Lett. 58 (1987) 1192.
[24] G. Binnig, N. Garcia, H. Rohrer, J.M. Soler, F. Flores, Phys. Rev. B 30 (1984) 4816.
[25] J.A. Stroscio, R.M. Feenstra, A.P. Fein, Phys. Rev. Lett. 58 (1987) 1668.
[26] J. Bardeen, Phys. Rev. Lett. 6 (1961) 57.
[27] J. Tersoff, D.R. Hamann, Phys. Rev. Lett. 50 (1983) 1998.
[28] J. Tersoff, D.R. Hamann, Phys. Rev. B 31 (1985) 805.
[29] R.M. Feenstra, J.A. Stroscio, A.P. Fein, Surf. Sci. 181 (1987) 95.
[30] M. Uda, et al., J. Electron Spectrosc. Relat. Phenom. 88–91 (1998) 643.
[31] N.D. Lang, W. Kohn, Phys. Rev. B 1 (1970) 4555.
[32] N.D. Lang, W. Kohn, Phys. Rev. B 3 (1971) 1215.
[33] H. Ishida, K. Terakura, Phys. Rev. B 36 (1987) 4510.